

Nodal $d + id$ pairing and topological phases on the triangular lattice: unconventional superconducting state of $\text{Na}_x\text{CoO}_2 \cdot y\text{H}_2\text{O}$

Sen Zhou^{1,2} and Ziqiang Wang¹

¹*Department of Physics, Boston College, Chestnut Hill, MA 02467 and*

²*National High Magnetic Field Laboratory, Florida State University, Tallahassee, FL 32310*

(Dated: May 27, 2019)

We show that finite angular momentum pairing, chiral superconductors on the triangular lattice have point zeroes in the complex gap function. A topological quantum phase transition takes place through a critical nodal superconducting state at a specific carrier density x_c where the normal state Fermi surface crosses these isolated zeros. For spin singlet pairing, we show that the second nearest neighbor $d + id$ -wave pairing can be the dominate superconducting channel. The gapless critical state at $x_c \simeq 0.25$ has six Dirac points and is topologically nontrivial with a T^3 spin relaxation rate below T_c . This picture provides a possible explanation for the unconventional superconducting state of $\text{Na}_x\text{CoO}_2 \cdot y\text{H}_2\text{O}$. We discuss the evolution of these topological phases with quantized spin Hall conductance and the phase transition as a function of Na doping.

PACS numbers: 74.20.-z, 74.20.Rp, 74.70.-b

The sodium cobaltate Na_xCoO_2 , a layered triangular lattice electron system, has received widespread interests since the recent discovery of the 5K superconducting (SC) phase in water intercalated $\text{Na}_x\text{CoO}_2 \cdot y\text{H}_2\text{O}$ near $x = 0.3$ [1]. While a very rich phase diagram is emerging over a broad range of Na concentrations [2], the nature of the superconducting phase has remained poorly understood. The main evidence that the SC phase is unconventional comes from the absence of the coherence peak in the NMR Knight shift at T_c and the power law temperature dependence (T^3) of the spin relaxation rate ($1/T_1$) below T_c [3, 4, 5]. Despite these evidence for an anisotropic SC gap function with line nodes, consistent with the specific heat [6] and μSR [7] measurements, there has been considerable debate over the pairing symmetry. Measurements of angle-averaged Knight shift in powdered samples have produced inconsistent results for both spin-triplet [8] and spin-singlet pairing [9]. The most recent measurements on high quality single crystals [10] show that the spin contributions to the Knight shift decreases below T_c along both the a and c -axis, strongly support that the Cooper pairs are formed in the spin-singlet state. In addition, both the Knight shift and the spin relaxation rate in the normal state indicate antiferromagnetic correlations in these high quality single crystals [5, 10].

On the theoretical side, there has been a growing number of proposals for unconventional superconductivity in the cobaltates. For spin-singlet pairing, the six-fold symmetry of the triangular lattice requires the low angular momentum paired state to have the chiral $d_{x^2-y^2} \pm id_{xy}$ symmetry, raising the exciting possibility of an unconventional, time-reversal symmetry breaking superconductor. Earlier studies that drew analogy to the high- T_c cuprates indeed found unanimously spin-singlet, $d + id$ pairing via the nearest neighbor antiferromagnetic superexchange in the triangular lattice t - J model at very

low doping [11, 12, 13, 14]. However, it is conventional wisdom that $d + id$ pairing, as well as other chiral paired states with complex order parameters, has a full gap and is thus inconsistent with NMR experiments [4, 5].

In this paper, we show that extended chiral paired states beyond the nearest neighbor (NN) have generic point zeroes in the complex gap function inside the first Brillouin zone. Consider a general (ℓ, n) -wave pairing with angular momentum ℓ of the pairs on the n -th NN bond. The complex pairing order parameter can be written down in real space for sites i and j ,

$$\Delta_{ij} = \Delta_{\ell n} e^{i\ell\theta_{ij}} \delta(\vec{r}_{ij} - \vec{R}_n), \quad (1)$$

where $\vec{r}_{ij} = \vec{r}_i - \vec{r}_j$, \vec{R}_n is the n -th NN lattice vector, and θ_{ij} the angle between the allowed \vec{r}_{ij} . The Fourier transform of Δ_{ij} defines the gap function $\Delta_{\ell n}(k)$ for (ℓ, n) -wave pairing and has the general form $\Delta_{\ell n}(k) = 2[\beta'_{\ell n}(k) + i\beta''_{\ell n}(k)]$. The real (β') and the imaginary (β'') parts of the gap function are given in Table I in terms of the triangular lattice harmonics for the chiral p -wave ($\ell = 1$) and d -wave ($\ell = 2$) cases. Nodes in the complex gap function arise where the real and imaginary parts of $\Delta_{\ell n}(k)$ vanish simultaneously, *i.e.* at the crossing points of the lines of zeroes of $\beta'(k)$ and $\beta''(k)$. Fig. 1 shows the locations of the gap nodes in the first Brillouin zone on the triangular lattice for the n -th NN chiral p and d -wave pairing. For first NN pairing, the nodes are pinned to the zone center and zone boundary and thus the generic chiral $(\ell, 1)$ -wave superconducting state has a full gap. Remarkably, for the case of $n > 1$, new nodes in the gap function appear *inside* the zone and can support nodal $(\ell, n > 1)$ -wave superconducting states.

Hereafter we focus on the singlet $d + id$ -wave case, *i.e.* chiral $(2, n)$ -paired states and argue that the existence of the nodes are relevant for understanding the superconducting state of hydrated cobaltates. For second NN pairing with $n = 2$, there are six nodes inside

Chiral p -wave pairing ($\ell = 1$):		
n	$\beta'_{1,n}(k)$	$\beta''_{1,n}(k)$
1	$\sqrt{3} \sin \frac{\sqrt{3}}{2} k_x \cos \frac{1}{2} k_y$	$\sin k_y + \cos \frac{\sqrt{3}}{2} k_x \sin \frac{1}{2} k_y$
2	$-\sqrt{3} \sin \frac{3}{2} k_y \cos \frac{\sqrt{3}}{2} k_x$	$\sin \sqrt{3} k_x + \cos \frac{3}{2} k_y \sin \frac{\sqrt{3}}{2} k_x$
3	$\sqrt{3} \sin \sqrt{3} k_x \cos k_y$	$\sin 2k_y + \cos \sqrt{3} k_x \sin k_y$

Chiral d -wave pairing ($\ell = 2$):		
n	$\beta'_{2,n}(k)$	$\beta''_{2,n}(k)$
1	$\cos k_y - \cos \frac{\sqrt{3}}{2} k_x \cos \frac{1}{2} k_y$	$\sqrt{3} \sin \frac{\sqrt{3}}{2} k_x \sin \frac{1}{2} k_y$
2	$\cos \sqrt{3} k_x - \cos \frac{3}{2} k_y \cos \frac{\sqrt{3}}{2} k_x$	$-\sqrt{3} \sin \frac{3}{2} k_y \sin \frac{\sqrt{3}}{2} k_x$
3	$\cos 2k_y - \cos \sqrt{3} k_x \cos k_y$	$\sqrt{3} \sin \sqrt{3} k_x \sin k_y$

TABLE I: Gap function $\Delta_{\ell n}(k) = 2[\beta'_{\ell n}(k) + i\beta''_{\ell n}(k)]$.

the zone marked by solid circles in Fig. 1b. They locate precisely at the six corners of the $\sqrt{3} \times \sqrt{3}$ zone boundary $\pm \mathbf{k}_{\alpha}^*$ with $\alpha = 1, 2, 3$, and $\mathbf{k}_1^* = 2\pi(2/3\sqrt{3}, 0)$, $\mathbf{k}_2^* = 2\pi(1/3\sqrt{3}, 1/3\sqrt{3})$, and $\mathbf{k}_3^* = 2\pi(1/3\sqrt{3}, -1/3\sqrt{3})$.

The first indication that this is special for the triangular lattice cobaltates comes from the fact that a single hexagonal Fermi surface (FS) at the superconducting concentration $x = 1/3$ coincides with the $\sqrt{3} \times \sqrt{3}$ zone boundary such that these nodes would lie directly on the FS. Recent angle-resolved photoemission (ARPES) experiments in the both the unhydrated [15, 16] and the hydrated [17] compound near $x \sim 0.3$ indeed observe a single hexagonal FS that coincides well with the $\sqrt{3} \times \sqrt{3}$ reduced zone boundary. This is highly unexpected since the Co^{4+} has 5 d -electrons occupying the lowest three t_{2g} orbitals. It turns out that strong correlation effects renormalize the crystal field splitting and bandwidths beyond the band theory predictions and produce a single quasiparticle band crossing the Fermi level as observed by ARPES experiments [18]. In Fig. 1b, we show the FS calculated in Ref. [18] at $x_c = 0.25$, which passes through the six gap nodes for the second NN $d + id$ -wave pairing. The value of x_c is smaller than $1/3$ due to the rounding of the hexagonal FS in both the ARPES data [15] and the theoretical calculations [18]. Interestingly, third NN $d + id$ -wave pairing introduces six nodes (Fig. 1b) at the corners of the 2×2 reduced zone, which intersects the FS close to $x = 1/2$ where the cobaltate is in an insulating phase with charge and spin order [2, 19].

The second, direct evidence for nodal $d + id$ -wave pairing at $x = x_c$ comes from the most recent NMR experiments. On high quality single crystals, Zheng *et al.* discovered that the T^3 decay of the relaxation rate $1/T_1$, *i.e.* the signature of line nodes in the gap function, is obeyed down to the lowest temperatures only at $x_c \simeq 0.26$, whereas deviations from T^3 are observed on both sides of x_c [5]. The existence of the Dirac nodes in the gap function at critical doping x_c for spin-singlet pairing on the triangular lattice strongly favors the scenario of second NN $d + id$ -wave pairing. In the following,

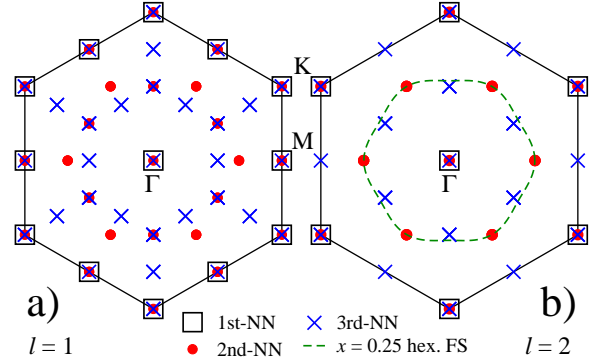


FIG. 1: Nodes of chiral (ℓ, n) -wave pairing where the gap function $\Delta_{\ell, n}(k)$ vanishes. (a) p -wave and (b) d -wave with normal state FS at $x = 0.25$ (dashed line).

we report a variational study of the $(2, n)$ -wave pairing states in an effective single-band $t-U$ model of the cobaltates, calculate the Knight shift and the spin relaxation rate $1/T_1$, and describe the topological properties of the superconducting phases.

The Hamiltonian is given on a triangular lattice,

$$H = \sum_{ij, \sigma} t_{ij} c_{i\sigma}^\dagger c_{j\sigma} + U \sum_i \hat{n}_{i\uparrow} \hat{n}_{i\downarrow} - \sum_{i,j} W_{ij} \hat{\Delta}_{ij}^\dagger \hat{\Delta}_{ij}, \quad (2)$$

where $c_{i\sigma}^\dagger$ creates a hole of spin σ with a Co on-site Coulomb repulsion U . To describe the a_{1g} band crossing the Fermi level, we consider up to third NN hopping with $t_{ij} = (t_1, t_2, t_3) = (-202, 35, 29)$ meV [19]. The hole density $n_i = 1 - x_i$ where x_i is the electron doping concentration. The last term in Eq. (2) is a phenomenological singlet pairing interaction $W_{ij} > 0$ between electrons on sites i and j with $\hat{\Delta}_{ij} = c_{i\uparrow} c_{j\downarrow} - c_{i\downarrow} c_{j\uparrow}$. The effects of strong correlation is accounted for in the Gutzwiller approximation, leading to a renormalized band dispersion,

$$\begin{aligned} \xi_k = & 2g_t t_1 (\cos k_y + 2 \cos \sqrt{3} k_x / 2 \cos k_y / 2) \\ & + 2g_t t_2 (\cos \sqrt{3} k_x + 2 \cos \sqrt{3} k_x / 2 \cos 3k_y / 2) \\ & + 2g_t t_3 (\cos 2k_y + 2 \cos \sqrt{3} k_x \cos k_y) - \mu, \end{aligned} \quad (3)$$

where $g_t = 2x/1 + x$ is the Gutzwiller renormalization factor in the large- U limit [19]. The variational BCS state for $(2, n)$ -wave pairing is given by

$$|\Psi_n\rangle = \prod_k |u_{nk}|^{1/2} \exp\left(\frac{1}{2} g_{nk} c_{k\uparrow}^\dagger c_{-k\downarrow}^\dagger\right) |0\rangle, \quad (4)$$

where $g_{nk} = v_{nk}/u_{nk} = -(E_{nk} - \xi_k)/\Delta_{nk}$ and the quasiparticle excitation energy $E_{nk} = \sqrt{\xi_k^2 + |\Delta_{nk}|^2}$. The gap function $\Delta_{nk} = 2W_n \Delta_n [\beta'_{2,n}(k) + \beta''_{2,n}(k)]$, with β given in Table I. The variational ground state is obtained by minimizing the energy with respect to Δ_n for a given W_n . In Fig. 2a, we compare Δ_n for the 1st, 2nd, and 3rd NN pairing with identical pairing strength $W_{1,2,3} = 50$ meV at several dopings. The 2nd NN $d + id$ pairing has the

largest pairing order parameter and thus the highest condensation energy. Including a NN Coulomb repulsion V [20] would further suppress the 1st NN pairing attraction W_1 , making the 2nd NN $d+id$ -wave pairing the dominate spin-singlet superconducting channel.

Next we turn to the properties of the second NN $d+id$ state. For our band parameters, the FS is circular and $x_c \simeq 0.19$. At $x = x_c$, the normal state FS crosses the six nodes of the gap function. Near $\pm\mathbf{k}_\alpha^*$, the quasi-particle dispersion E_k (hereafter we drop the index n) has a conical spectrum. For example, expanding around $\pm\mathbf{k}_1^*$, $E_k \simeq \sqrt{(A^2 + B^2)(k_x \mp 4\pi/3\sqrt{3})^2 + B^2 k_y^2}$, with $A = 3(t_1 - 2t_3)$ and $B = 9W\Delta/2$. Thus, the six nodes are described by three pairs of Dirac fermion doublets with anisotropic velocities, which govern the properties of low energy excitations. We calculate the tunneling density of states (DOS) $N(E)$ and the temperature dependence of the ab -plane Knight shift (K_s) and the spin relaxation rate ($1/T_1$) according to

$$\left[K_s, \frac{1}{T_1} \right] \propto - \int_{-\infty}^{\infty} [1, TN(E)] N(E) \frac{\partial f(E)}{\partial E} dE. \quad (5)$$

The results are plotted in Figs. 2b-d. The calculated $N(E)$ shows a linearly vanishing, V-shaped DOS at $x = x_c$ analogous to $d_{x^2-y^2}$ -wave pairing on the square lattice. As a consequence, the Knight K_s and $1/T_1$ follows the T and T^3 behaviors below T_c in excellent agreement with the NMR experiments on single crystals at $x \simeq 0.26$ [5, 10]. For $x \neq x_c$, the normal state FS does not overlap the nodes in the gap function. Fig. 2b shows that at $x = 0.4$ the DOS is fully gapped at low energies, but restores to the V-shape above the energy gap. This leads to a rapid crossover of K_s and $1/T_1$ from the respective T and T^3 behaviors near T_c to exponential decays at low temperatures as shown in Figs. 2c and 2d. In the presence of disorder, we expect that disorder-induced filling of the DOS gap to produce a constant K_s and a linearly vanishing $1/T_1$ at low temperatures [4].

We now discuss the topological properties of the second NN $d+id$ -wave superconducting phases and the topological quantum phase transition as the carrier density x evolves across x_c . The topological order in chiral fermion-paired states has been a subject of growing interests in connection to unconventional superconductors/superfluids and quantum Hall states [21, 22, 23]. The key point is that the complex order parameter and dispersion ξ_k forms a unit pseudospin vector introduced by Anderson [24]: $\mathbf{m}(k) = (\text{Re}\Delta_k, -\text{Im}\Delta_k, \xi_k)/E_k$. Since $|\mathbf{m}|^2 = 1$, \mathbf{m} lives on a 2-sphere S^2 . The superconducting state can be viewed as a BCS mapping from \mathbf{k} -space, which is also a S^2 (compactified from a torus in our case), to the pseudospin S^2 . This is evident when we write \mathbf{m} in term of the pairing function $g_k = v_k/u_k$ in Eq. (4),

$$m_1(k) + im_2(k) = \frac{2g_k}{1 + |g_k|^2}, \quad m_3(k) = \frac{1 - |g_k|^2}{1 + |g_k|^2}. \quad (6)$$

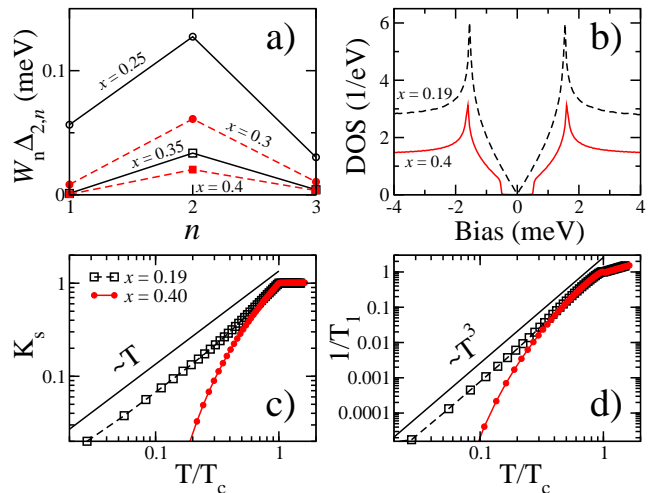


FIG. 2: (a) Comparison of $d+id$ pairing order parameters at several dopings for $W_{1,2,3} = 50$ meV. (b-d) Properties of 2nd NN $d+id$ -wave pairing at $x = 0.19 = x_c$ for $W_2 = 50$ meV and $x = 0.4 > x_c$ for $W_2 = 73$ meV: Tunneling DOS (b), temperature dependence of Knight shift K_s (c) and NMR relaxation rate $1/T_1$ (d) normalized by their values at T_c .

Such maps are classified by the homotopy classes in terms of a topological winding number Q . We write the lattice version of Q ,

$$Q = \frac{1}{8\pi} \sum_{\Delta} \mathbf{m}(k_1) \cdot [\mathbf{m}(k_2) \times \mathbf{m}(k_3)], \quad (7)$$

where the summation is over all elemental triangular plaquettes with corners labeled as 1, 2, 3. Topologically distinct phases are categorized by different winding numbers Q that counts the number of times the pseudospin configuration \mathbf{m} wraps around the sphere. We find that $Q \neq 0$ if g_k has a *singular* vortex structure around the nodes of the complex gap function, a condition that depends on the location of the FS. In Fig. 3, we show the calculated Q for the second NN $d+id$ pairing at $x > x_c$, $x < x_c$ and the critical state at $x = x_c$. All of them are topologically nontrivial. For $x > x_c$, the normal state FS encloses only the gap node at the zone center, around which $g_k \propto 1/(k_x - ik_y)^2$, exhibiting a singular ($\ell = 2$) double vortex. This charge-two magnetic monopole contributes two flux quanta to the surface integral and gives $Q = \mp 2$ (Fig. 3) for such fully gapped topological phase. The sign corresponds to the relative sign of the real and imaginary parts of the order parameter. Note that near the gap nodes outside the FS, g_k behaves as zeroes, e.g. $g_k \propto (k_x \mp 4\pi/3\sqrt{3}) + ik_y$ near the nodes at $\pm\mathbf{k}_1^*$, and thus do not contribute to the winding number. As the electron doping is reduced to $x < x_c$, the normal state FS now encloses, in addition to the node at Γ , the six nodes due to second NN pairing where g_k exhibits singular vortex structure, e.g. $g_k \propto 1/(k_x \mp 4\pi/3\sqrt{3} + ik_y)$ near $\pm\mathbf{k}_1^*$. Each pair of the nodes can be viewed as a singular double

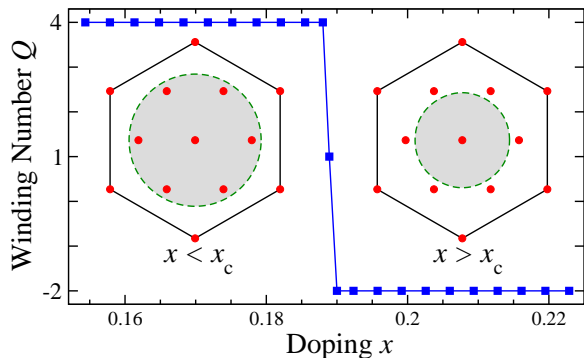


FIG. 3: Topological winding number as a function of doping in the second NN $d + id$ -wave superconducting state. Insets show the locations of the nodes in the complex gap function and the normal state FS.

vortex. The contribution to the magnetic flux through the sphere is thus increased by six flux quanta leading to $Q = \pm 4$ as shown in Fig. 3.

In the critical state at $x = x_c$, the FS passes through the six gap nodes. The pseudospin vector \mathbf{m} is not well defined exactly at these isolated diabolic points, which are removed from the summation in Eq. (7). Remarkably, Fig. 3 shows that the winding number $Q = \pm 1$ and the critical state is gapless topologically nontrivial state. This suggests that each pair of the gap nodes in the critical state contributes a single vortex in k -space, reminiscent of the situation in the $p + ip$ state [23, 25]. Indeed, evaluating Q in the continuum limit along the line integrals of the six circles cutting out the nodes at \mathbf{k}_α^* , one finds that each of the latter contributes half a magnetic flux leading to the total $Q = \pm 1$. We note that the existence of such a *gapless* topological phase in two dimensions is new and consistent with the view point that gapless fermions emerge as a result of a form of quantum order [26] in the critical state. Physically, the topological invariant winding number Q corresponds to the quantization of the spin Hall conductance σ_{xy}^s [22, 23]. In unit of the spin conductance quantum $(\hbar/2)^2/2\pi\hbar$, the spin Hall conductance is $\sigma_{xy}^s = Q$. Thus, we predict that as the electron doping x evolves across x_c , the superconducting state of the cobaltate exhibits quantum spin Hall transitions from ∓ 2 to ± 4 with quantized critical spin Hall conductance ± 1 . We expect novel properties associated with the edge states.

In summary, we have proposed a class of nodal chiral superconductors. The spin-singlet, second NN $d + id$ -wave pairing turns out to be consistent with the NMR experiments on high quality single crystals of hydrated cobaltate superconductors, and has some remarkable topological properties related to the quantum spin Hall transitions. Although the microscopic origin for second NN $d + id$ pairing is beyond our scope here, it is conceivable that (i) a strong NN Coulomb repulsion [20], (ii) a larger 2nd NN superexchange, and (iii) the frustration of

the NN AF correlation on the triangular lattice and the proximity to inhomogeneous charge/spin ordered state [19, 20] will favor a dominant extended pairing interaction beyond the first NN. It is noted that the chiral pairing state breaks time-reversal symmetry which should in principle be detectable by μ SR or optical Kerr experiments with sufficient resolution. The orbital current near a unitary impurity produces a static magnetic field. To estimate the size of the field, we performed self-consistent calculations for the circulating current near a unitary impurity. The maximum current around the impurity site is ~ 100 nA for a pairing strength $W_2 = 50$ meV corresponding to a $T_c \sim 5$ K. This gives an estimate of the magnetic field at the impurity site ~ 1 G, which is close to the upper bound set by the earlier μ SR experiments [27, 28]. Future experiments are very desirable to determine whether time-reversal symmetry is broken in the superconducting cobaltates.

We are grateful to Y. Yu for many useful discussions. This work was supported by DOE grant DE-FG02-99ER45747.

-
- [1] K. Takada, *et al.*, Nature (London) **422**, 53 (2003).
 - [2] M. L. Foo, *et al.*, Phys. Rev. Lett. **92**, 247001 (2004).
 - [3] K. Ishida, *et al.*, J. Phys. Soc. Jpn, **72**, 3041 (2003).
 - [4] T. Fujimoto, *et al.*, Phys. Rev. Lett. **92**, 047004 (2004).
 - [5] G.-q. Zheng, *et al.*, J. Phys.: Condens. Matter **18**, L63 (2006).
 - [6] H. D. Yang, *et al.*, Phys. Rev. B **71**, 020504 (2005).
 - [7] A. Kanigel, *et al.*, Phys. Rev. Lett. **92**, 257007 (2004).
 - [8] M. Kato, *et al.*, J. Phys.: Condens. Matter **18**, 669 (2006).
 - [9] Y. Kobayashi, *et al.*, J. Phys. Soc. Jpn. **74**, 1800 (2005).
 - [10] G.-q. Zheng, *et al.*, Phys. Rev. B **73**, 180503 (2006).
 - [11] G. Baskaran, Phys. Rev. Lett. **91**, 097003 (2003).
 - [12] B. Kumar and B. S. Shastry, Phys. Rev. B **68**, 104508 (2003).
 - [13] M. Ogata, J. Phys. Soc. Jpn. **72**, 1839 (2003).
 - [14] Q.-H Wang, D.-H Lee, and P. A. Lee, Phys. Rev. B **69**, 092504 (2004).
 - [15] H.-B. Yang, *et al.*, Phys. Rev. Lett. **95**, 146401 (2005); Phys. Rev. Lett. **92**, 246403 (2004).
 - [16] M. Z. Hasan, *et al.*, Phys. Rev. Lett. **92**, 246402 (2004).
 - [17] T. Shimojima, *et al.*, Phys. Rev. Lett. **97**, 267003 (2006).
 - [18] S. Zhou, *et al.*, Phys. Rev. Lett. **94**, 206401 (2005).
 - [19] S. Zhou and Z. Wang, Phys. Rev. Lett. **98**, 226402 (2007).
 - [20] O. I. Motrunich and P. A. Lee, Phys. Rev. B **69**, 214516 (2004); **70**, 024514 (2004).
 - [21] G.E. Volovik, JETP Lett. **66**, 522 (1997).
 - [22] T. Senthil, J.B. Marston, and M.P.A. Fisher, Phys. Rev. B **60**, 4245 (1999).
 - [23] N. Read and D. Green, Phys. Rev. B **61**, 10267 (2000).
 - [24] P.W. Anderson, Phys. Rev. **110**, 827; **112**, 1900 (1958).
 - [25] G.E. Volovik, Sov. Phys. JETP **67**, 1804 (1988).
 - [26] X. G. Wen and A. Zee, Phys. Rev. B **66**, 235110 (2002).
 - [27] W. Higemoto, *et al.*, Phys. Rev. B **70**, 134508 (2004).
 - [28] Y. J. Uemura, *et al.*, arXiv:cond-mat/0403031 (2004).